Naval Research Laboratory

Washington, DC 20375-5320

NRL/MR5620--99-8195

POTDR Measurements on Buried Optical Fibers

KENT B. HILL
CARL A. VILLARRUEL

Optical Techniques Branch
Optical Sciences Division

August 14, 1998

REPORT DOCUMENTATION PAGE

Form Approved
OMB No. 0704-0188

1. AGENCY USE ONLY *(Leave Blank)*

2. REPORT DATE
August 14, 1998

3. REPORT TYPE AND DATES COVERED

4. TITLE AND SUBTITLE
POTDR Measurements on Buried Optical Fibers

5. FUNDING NUMBERS

6. AUTHOR(S)
Kent B. Hill and Carl A. Villarruel

7. PERFORMING ORGANIZATION NAME(S) AND ADDRESS(ES)
Naval Research Laboratory
Washington, DC 20375-5320

8. PERFORMING ORGANIZATION REPORT NUMBER
NRL/MR/5620--98-8195

9. SPONSORING/MONITORING AGENCY NAME(S) AND ADDRESS(ES)
DARPA

10. SPONSORING/MONITORING AGENCY REPORT NUMBER

11. SUPPLEMENTARY NOTES

12a. DISTRIBUTION/AVAILABILITY STATEMENT
Approved for public release; distribution unlimited.

12b. DISTRIBUTION CODE
A

13. ABSTRACT *(Maximum 200 words)*

In this report, a polarization-sensitive optical time domain reflectometer (POTDR) is described and results of POTDR measurements on buried optical fibers in a network testbed are presented. The polarization effects observed on different fibers in the testbed show that the birefringence may vary significantly in fibers of the same type and the same cable. Measurements taken over several hours indicate that polarization effects in buried optical fibers are quite stable.

14. SUBJECT TERMS
OTDR
Polarization

15. NUMBER OF PAGES
22

16. PRICE CODE

17. SECURITY CLASSIFICATION OF REPORT	18. SECURITY CLASSIFICATION OF THIS PAGE	19. SECURITY CLASSIFICATION OF ABSTRACT	20. LIMITATION OF ABSTRACT
UNCLASSIFIED	UNCLASSIFIED	UNCLASSIFIED	UL

NSN 7540-01-280-5500

Standard Form 298 (Rev. 2-89)
Prescribed by ANSI Std 239-18
298-102

CONTENTS

1. INTRODUCTION 1

2. THEORY 2

3. EXPERIMENTAL SETUP 3

4. EXPERIMENTAL RESULTS 4

5. CONCLUSIONS 8

6. LIST OF REFERENCES 9

APPENDIX A—FIBER CABLE CONSTRUCTION 11

APPENDIX B—DATA 13

POTDR Measurements on Buried Optical Fibers

KENT B. HILL AND CARL A. VILLARRUEL

1. Introduction

Optical time-domain reflectometry (OTDR) was first demonstrated in 1976 to measure the attenuation properties of optical fibers[1]. An OTDR launches a short pulse of light into the end of a fiber, and measures the intensity of Rayleigh-backscattered light as a function of time. Light that is backscattered from the input pulse at a distance d from the end of the fiber arrives at the detector at time $2d/v$, where v is the velocity of light in the fiber. Thus, the time dependence of the measured signal corresponds to the distance traveled by the pulse in the fiber, and the intensity of the signal is a measure of the attenuation encountered in the fiber. Fresnel reflections from connectors, splices, or breaks in the fiber produce spikes in the signal that make such reflections easy to locate. Discrete losses on the fiber appear as discontinuities in the OTDR signal making it possible to locate and measure the loss of discrete components or anomalies on the fiber. Because of their utility for measuring the properties of optical fibers, OTDRs are widely used in various applications such as fiber production, network testing, and fiber-optic sensors.

By placing a polarization analyzer in the path of the receiver of an OTDR, polarization effects in optical fibers can be measured. Polarization-OTDR (POTDR) techniques were first developed to measure the effects of external fields acting on a fiber[2]. Recently, POTDR techniques have been developed to characterize polarization mode dispersion (PMD) in optical fibers[3-5]. A POTDR that measures the complete state-of-polarization (SOP) of backscattered light has been demonstrated for the measurement of linear birefringence and twist-induced circular birefringence in a fiber[6]. Such measurements can also be used to measure polarization dependent losses of fiber-optic components and other anomalies in a fiber. In order to make such measurements in an installed fiber-optic network, polarization effects due to environmental conditions must be negligible. Polarization fluctuations in installed submarine[7-8] and terrestrial[9-11] fiber cables have been observed in end-to-end polarization measurements, but, to our knowledge, polarization effects as a function of position in such cables have not been measured. To determine the environmental stability of polarization effects in installed fiber networks, POTDR measurements were recently taken on buried fibers in a network testbed. In this report, results of these measurements are presented, and it is shown that environmental effects on polarization in buried fibers can be neglected over time periods extending from several minutes to hours. In Section 2, a brief theoretical discussion of POTDR measurements is presented. In Section 3, the experimental POTDR setup and the network testbed are described, and in Section 4, experimental results are presented. Finally, in Section 5, conclusions are drawn.

Manuscript approved July 8, 1998.

2. Theory

The four Stokes parameters characterizing the SOP of the backscattered light in an OTDR experiment can be determined from four measurements with different polarization analyzers placed in front of the receiver[12]. These measurements can be taken with no polarization analyzer, two linear polarizers oriented at 0° and 45°, and a circular polarizer consisting of a quarter-wave plate followed by a linear polarizer oriented 45° from the axis of the wave plate. If $I_i, i = 1, \ldots, 4$ are the total intensity and the intensities through the horizontal, diagonal, and circular polarizers, respectively, then the Stokes parameters are given by

$$I = I_1,$$
$$M = 2I_2 - I_1,$$
$$C = 2I_3 - I_1,$$

and

$$S = 2I_4 - I_1. \tag{1}$$

Light propagating in a single-mode fiber can be decomposed into two orthogonal polarization modes[13]. In a fiber with perfect circular symmetry, these modes are degenerate, and they propagate at the same velocity. However, in any real fiber, this symmetry is broken by geometrical deformations and material anisotropies that can be caused by various elastooptic, magnetooptic, and electrooptic effects. These effects cause the polarization eigenmodes of the fiber to propagate with different phase velocities, and the difference in the propagation constants $\Delta\beta = \omega\Delta n / c$ is known as birefringence, where Δn is the difference in the effective refractive index for the two modes. On the Poincaré sphere, birefringence is directed along the axis of the SOP of the polarization eigenmodes. The SOP of light propagating in the fiber rotates about this axis at a rate proportional to the magnitude of the birefringence. Uniform birefringence causes the SOP of light to evolve through a periodic sequence of states as it propagates through a fiber. Linear birefringence causes retardation and circular birefringence causes rotation of the SOP. If the direction of birefringence is non-uniform along the length of a fiber, then coupling between polarization modes occurs, and the SOP evolves through all possible states. The correlation length l_c is defined to be the length of fiber at which $1/e^2$ of the power in one mode is coupled to the other. This parameter is highly sensitive to mechanical stresses which are typically greater on spooled fibers than on cabled fibers.

The dispersion caused by birefringence in a fiber is known as PMD. We define PMD as the delay time $\Delta\tau$ that is encountered between polarization eigenmodes propagating a distance L through the fiber. For short lengths of fiber, polarization mode coupling is weak, and PMD is derived from the differential group velocity as follows:

$$\Delta\tau = L\frac{d\Delta\beta}{d\omega} = \frac{L}{c}\left(\Delta n - \omega\frac{d\Delta n}{d\omega}\right). \tag{2}$$

It can be seen that the short-length PMD scales linearly with the length of the fiber. For lengths of fiber longer than the correlation length (typically ~100 m), mode-coupling effects cause PMD to scale with the square root of fiber length. In this case, PMD is related to the statistical properties of the local birefringence along the fiber to obtain[14]

$$\langle \Delta\tau^2 \rangle = \left(\frac{d\Delta\beta}{d\omega} \right)^2 Ll_c, \quad L >> l_c. \tag{3}$$

It has been shown that polarization mode coupling causes light emitted from a spectrally broad bandwidth source to become depolarized as it propagates through a fiber[13,15]. This depolarizing effect becomes significant when the total PMD is greater than the coherence time of the source. Therefore, the coherence time of the source used in a POTDR should be chosen to exceed the total PMD that will be encountered in a fiber.

In a POTDR, the effects of birefringence can be measured as a function of distance in the fiber. The beat length of a fiber is defined to be the length of fiber that produces a 360° phase shift between the two polarization eigenmodes. Weak birefringence (long beat length) in a fiber causes the SOP of the backscattered light to change slowly in a POTDR measurement, while strong birefringence (short beat length) causes a rapid change. The spatial resolution of an OTDR is limited to half the spatial width of the input pulse due to convolution of the input with the impulse response of the fiber. Therefore, the spatial pulsewidth used for a POTDR measurement must be much shorter than the beat length in order to resolve changes in the SOP. The SOP of the input pulse also affects POTDR measurements because it determines the amount of light launched in each of the polarization eigenmodes of the fiber. The evolution of the SOP in a POTDR measurement depends on the amount of light launched in these modes. For example, in the absence of mode coupling, the SOP of light launched in one eigenmode of a uniformly birefringent fiber does not change while the SOP of light launched equally in both eigenmodes rotates around a great circle on the Poincaré sphere.

3. Experimental Setup

The experimental POTDR setup is shown in Fig. 1. An EXFO FCS-300 1310/1550 nm dual wavelength OTDR PC card was modified to provide direct access to

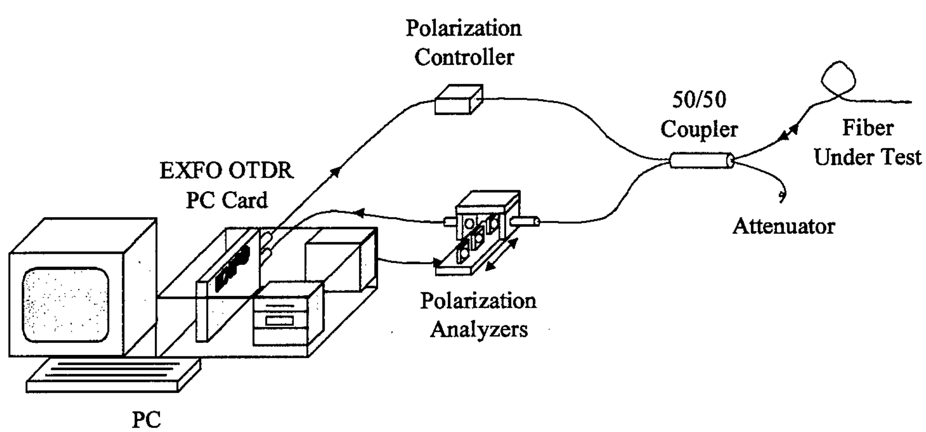

Fig. 1. Experimental POTDR setup.

the laser output port and the photoreceiver port. A liquid-crystal polarization controller was inserted at the laser output to control the state-of-polarization (SOP) of the input pulses. A fiber-to-fiber coupler was inserted in the path of the receiver, and a computer-controlled translation stage was used to move any one of three polarization analyzers into the path of the collimated beam. Two linear polarizers oriented at 0° and 45°, and a circular polarizer were used to measure the SOP as described in Section 1.

The network testbed consisted of three cables of optical fiber that ran together through a series of underground cable ducts and into a buried loop around the test facility. One cable contained 52 dispersion shifted fibers, half manufactured by AT&T and half by Corning. This cable was of the *Lightpack* LXE design (see Appendix A) and had a total length of about 5 km. Another cable contained 96 standard single-mode fibers and was a *Lightpack* RL type design with a total length of 6 km. The third cable contained 144 standard fibers in a ribbon NM construction and was about 6 km in length. Longer fiber lengths were created by splicing 5 km segments of fiber together at the ends of the cables. At one point in the test loop, the cables had been cut by a backhoe, and the fibers had been repaired with splices. Most of the splices were fusion splices, but some mechanical splices were used at the repair point.

4. Experimental Results

For our tests, measurements were taken on several different fibers during the daytime, and two automated overnight measurements were taken on a particular fiber. The overnight measurements were scheduled to repeat every 12 minutes in order to evaluate the environmental stability of the observed polarization effects. A typical POTDR measurement is shown in Fig. 2. This measurement was taken on a fiber consisting of four segments of AT&T 5D fiber in a *Lightpack* cable. It can be seen that the magnitude of the polarization effects in different fiber segments varied. Similar measurements on other fibers are included in Appendix B. These POTDR measurements are similar to measurements taken on fiber test spools in the laboratory. Measurements taken with different input SOPs are plotted in Fig. 3. The input SOPs given by $\mathbf{P}_1$, $\mathbf{P}_2$, and $\mathbf{P}_3$ were not measured, but they were chosen to produce noticeable changes in the measurements. It can be seen that the relative intensity of the backscattered light

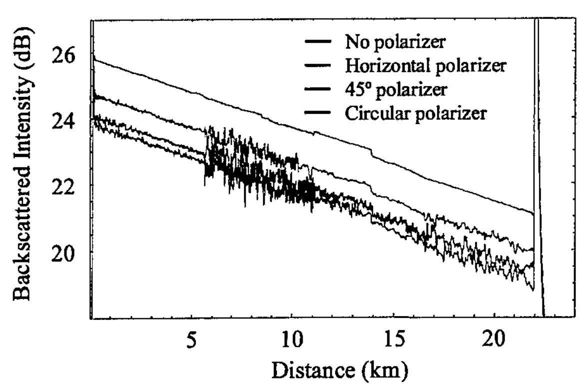

Fig. 2. Typical POTDR measurement.

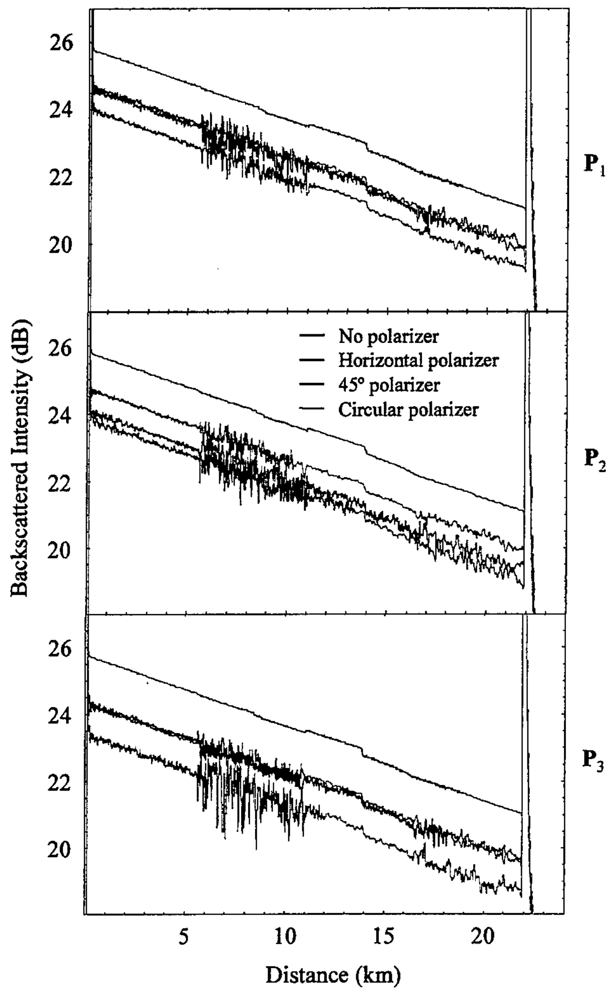

Fig. 3. POTDR measurements with different input SOPs.

measured through the different polarizers changed with the input SOP; however, the magnitude of the polarization effects was consistently greater on certain fibers than on others.

One explanation for the different magnitudes of polarization effects on different fiber segments is that the resolution of the measurements was not good enough to resolve the effects on some fiber segments. This would indicate that the birefringence of those segments was higher than that of the other segments. In all of our measurements, 275 ns pulses were used, corresponding to a resolution of about 30 meters. When shorter pulses were used, the resolution of the polarization effects did not seem to improve; however, this may have been due to automatic gain control in the OTDR card that caused a reduction in the bandwidth of the measurements when the gain was increased. The gain setting of the OTDR card often changed in the middle of a single measurement to compensate for losses due to attenuation in the fiber. This effect can be seen in Fig. 4, where a blown up section of two successive POTDR measurements is shown. The two measurements were identical except that the OTDR card adjusted the gain during one of

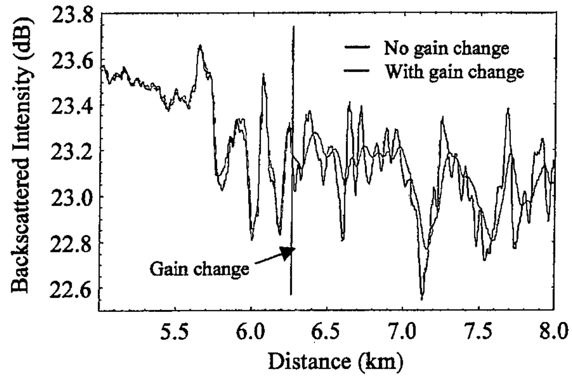

Fig. 4. Effect of automatic gain control on POTDR measurements.

them. The vertical line is drawn where the bandwidth of the measurement was reduced due to the change in gain. This behavior of the OTDR card was discovered after returning from the field tests while analyzing the data. There was no way to control the gain, and its changes were not predictable.

As seen in Eq. (3), the long-length PMD of a fiber with fixed Ll_c scales with the derivative of the birefringence with respect to frequency. PMD measurements of several fiber segments installed in the testbed were compared with our POTDR measurements to determine whether the PMD measurements could be correlated with the polarization effects that were observed (see Appendix B). No correlation was observed; however, the conditions under which the PMD measurements were made were unknown, and inaccuracies may exist due to changes in birefringence induced by the cabling process and environmental stresses applied to the installed cables.

It is expected that depolarization of POTDR pulses due to polarization mode coupling would cause the magnitude of the measured polarization effects to decrease with distance in the fiber. Measurements were taken from both ends of a fiber, and the magnitude of the polarization effects on any given segment of the fiber was the same in both measurements. Although the spectral width of the POTDR source was rather broad (~15 nm), any depolarization of the POTDR signal did not significantly affect our measurements.

The birefringence of a fiber is very sensitive to physical perturbations and environmental changes. By making successive POTDR measurements, we could determine the stability of the polarization effects over time. Plots of overnight POTDR measurements are shown in Fig. 5. The polarization effects observed in these measurements did not change significantly during the entire measurement period. Density plots of the measurements for each of the three polarization filters are shown in Fig. 6. A few discontinuities appear in the measurements through the horizontal filter, but these are due to gain changes in the OTDR. A small, gradual change in the polarization can be seen over the first two hours, and again near the end of the measurements. These changes occur near sunset and sunrise suggesting that they may be temperature induced. A temperature recorder was placed in one of the manholes along

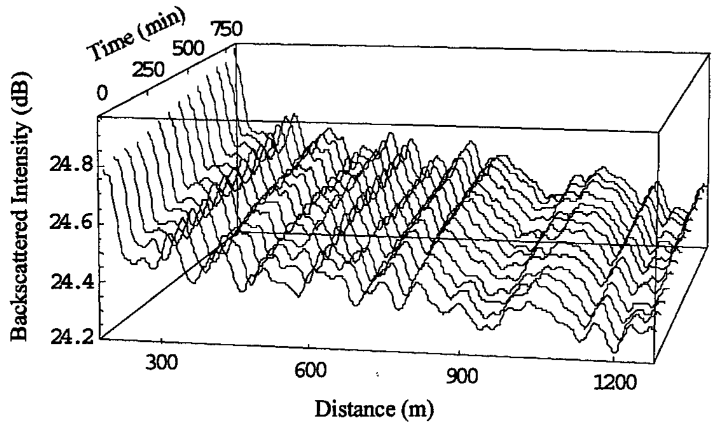

Fig. 5. Overnight POTDR measurements.

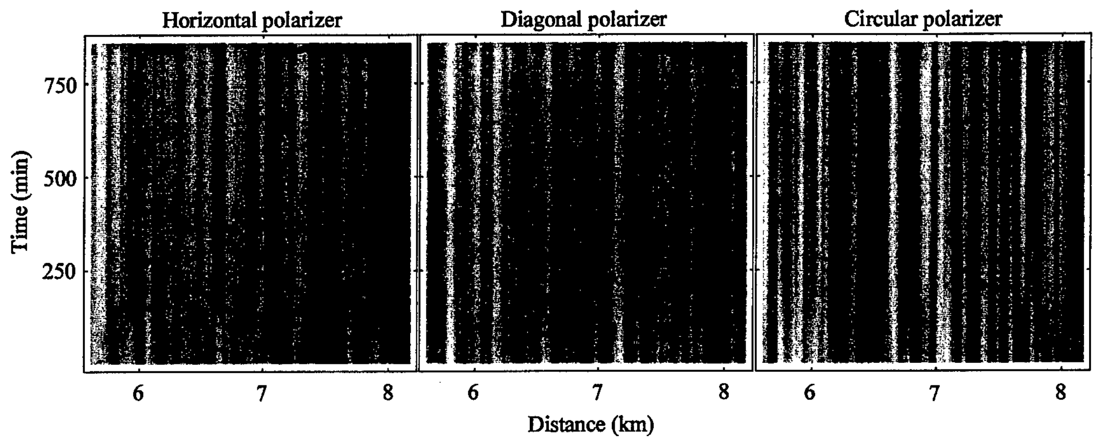

Fig. 6. Density plots of overnight POTDR measurements.

the route of the fiber to record any changes in temperature. The weather was consistently warm and humid, and the temperature inside the manhole only varied by ~1° during all of our measurements. Any effects of vehicle traffic along roads traversing the path of the fibers were unnoticeable; however, the fibers were well isolated from vibrations inside the cable ducts.

During analysis of our measurements, it was found that the complete SOP could not be determined accurately due to several problems in the measurements. First, it was found that the circular polarizer used in the measurements was improperly aligned by the manufacturer. An attempt was made to correct the data using the measured alignment of the polarizer, but the Stokes analysis still produced invalid results. New measurements were taken in the lab with a good set of polarizers, and it was found that 10 ns (1 m) pulsewidths were necessary to resolve polarization effects in the fiber spools tested. The dynamic range of the OTDR at this pulsewidth was not good enough to accurately determine the SOP. Because the measurements at the field site were taken with 275 ns pulses and because of problems with the gain control, the resolution of the measurements was insufficient for accurate SOP analysis. In future work, efforts will be made to improve these measurement errors; however, it appears that data from a single polarizer may be sufficient to characterize many polarization effects in optical fibers.

5. Conclusions

We have shown that polarization effects measured by a POTDR on buried optical fibers can be quite stable. The effects measured in the field were similar to effects measured on fiber spools in the lab. In the environment that we tested, POTDR measurements did not change significantly over time periods of several hours. However, this stability may be attributed to the benign environmental conditions present during our experiments. Further measurements are needed to determine the impact of more severe environments on POTDR measurements. Because of the environmental stability of our measurements, the use of POTDR measurements to characterize polarization effects in fiber networks appears to be a useful technique.

List of References

1. M. K. Barnoski and S. M. Jensen, "Fiber waveguides: a novel technique for investigating attenuation characteristics," *Appl. Opt.* **15**, 2112-2115 (1976).

2. A. J. Rogers, "Polarization-optical time domain reflectometry: a technique for the measurement of field distributions," *Appl. Opt.* **20**, 1060-1074 (1981).

3. A. M. Vengsarkar and L. G. Cohen, "Polarization optical time domain reflectometry for statistical evaluation of polarization mode dispersion," *Electron. Lett.* **29**, 848-850 (1993).

4. A. Tardy, M. Jurczyszyn, F. Bruyere, and M. Hertz, "Fiber PMD Analysis for optical-fiber cable using polarization OTDR," in *Optical Fiber Communication Conference*, 1995 OSA Technical Digest Series (Optical Society of America, Washington, D.C., 1995), paper ThD2.

5. A. J. Rogers, Y. R. Zhou, and V. A. Handerek, "Computational polarization-optical time domain reflectometry for measurement of the spatial distribution of PMD in optical fibers," in *4th Optical Fiber Measurement Conference, OFMC '97* (1997), pp. 126-129.

6. J. G. Ellison and A. S. Siddiqui, "A fully polarimetric optical time-domain reflectometer," *IEEE Photon. Technol. Lett.* **10**, 246-248 (1998).

7. Y. Namihira, S. Ryu, M. Kuwazuru, K. Mochizuki, and Y. Iwamato, "Polarization fluctuation of submarine-cabled single-mode optical fibers in ocean installation," *Electron. Lett.* **23**, 343-344 (1987).

8. C. D. Poole, N. S. Bergano, R. E. Wagner, and H. J. Shulte, "Polarization dispersion and principal states in a 147-km undersea lightwave cable," *J. Lightwave Technol.* **6**, 1185-1190 (1988).

9. R. A. Harmon, "Polarisation stability in long lengths of monomode fiber," *Electron. Lett.* **18**, 1058-1060 (1982).

10. L. Giehmann and M. Rocks, "Measurement of polarization fluctuations in installed single-mode optical fiber cables," *Opt. And Quantum Electron.* **19**, 109-113 (1987).

11. G. Nicholson and D. J. Temple, "Polarization fluctuation measurements on installed single-mode optical fiber cables," *J. Lightwave Technol.* **7**, 1197-1200 (1989).

12. D. Clarke and J. F. Grainger, *Polarized Light and Optical Measurement* (Pergamon Press Ltd., Oxford, 1971), Ch. 4.

13. S. C. Rashleigh, "Origins and control of polarization effects in single-mode fibers," *J. Lightwave Technol.* **LT-1**, 312-331 (1983).

14. C. D. Poole and J. Nagel, "Polarization effects in lightwave systems" in *Optical Fiber Telecommunications IIIA*, I. P. Kaminow and T. L. Koch, eds. (Academic Press, San Diego, 1997), Ch. 6.

15. W. K. Burns, R. P. Moeller, and C. Chen "Depolarization in a single-mode optical fiber," *J. Lightwave Technol.* **LT-1**, 44-50 (1983).

Appendix A
Fiber Cable Construction†

The basic building block of a *Lightpack* cable core is a bundle of 2 to 12 fibers held together loosely with two helically applied binders. The *Lightpack* cable core consists of an extruded plastic tube, filled with filling compound and containing up to eight fiber bundles (up to 96 fibers). The cross-section of a *Lightpack* cable core is shown in Fig. A1.

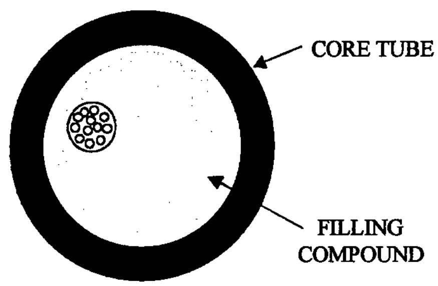

Figure A1. *Lightpack* cable core.

The construction of the LXE-ME sheath is shown in Fig. A2. An overlapped armor layer of 0.15 mm (0.006 in) corrugated electrolytic chrome coated steel (ECCS) envelopes the core tube and has a ripcord under it to ease its removal. The steel armor is coated to inhibit corrosion and to bond to the outer jacket. Two steel wire strength members run longitudinally along the armor, diametrical from each other. A ripcord is located next to each steel wire for ease of sheath removal. The sheath is completed with a black high-density polyethylene (HDPE) jacket.

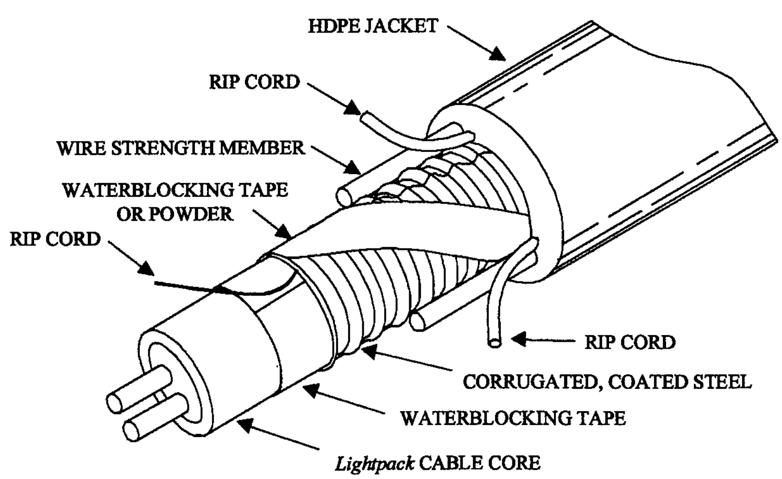

Figure A2. LXE-ME Sheath

†Descriptions taken from "Lucent Technologies Fiber Optic Outside Plant Cable."

The Primary RL sheath is shown in Fig. A3. An overlapped armor layer of 0.13 mm (0.005 in) corrugated stainless steel envelopes the core tube and has a ripcord under it to ease its removal. The armor is coated to promote bonding to the outer jacket. The armor application is followed by a single helical application of fourteen 0.53 mm (0.021 in) diameter steel wires and a black HDPE jacket.

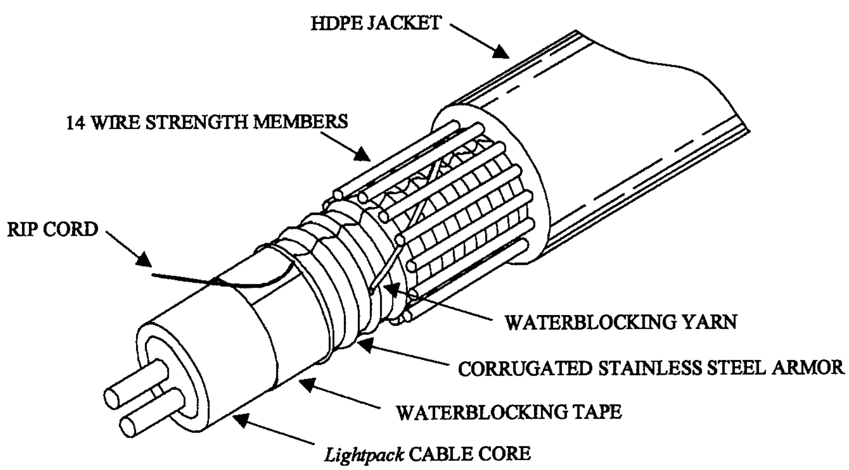

Figure A3. Primary RL Sheath

Appendix B
Data

The following plots are samples of data collected from the various fibers in the network testbed. Results from previously taken PMD measurements are included where available. The conditions under which the PMD measurements were taken are unknown.

Data set: WMR5D210
AT&T 5D fiber in *Lightpack* cable

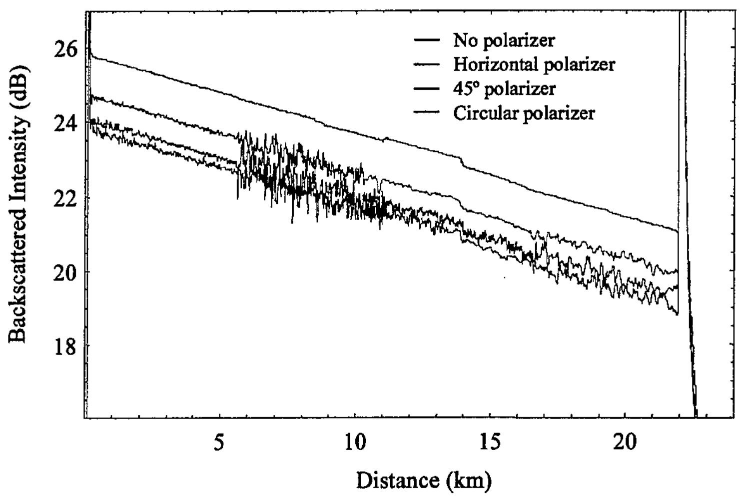

Wavelength: 1550 nmPulsewidth: 275 ns

←.261→←.033→←.000→←.033→

PMD measured before fiber installation (ps/km$^{1/2}$)

Data set: WMR5D211
AT&T 5D fiber in *Lightpack* cable

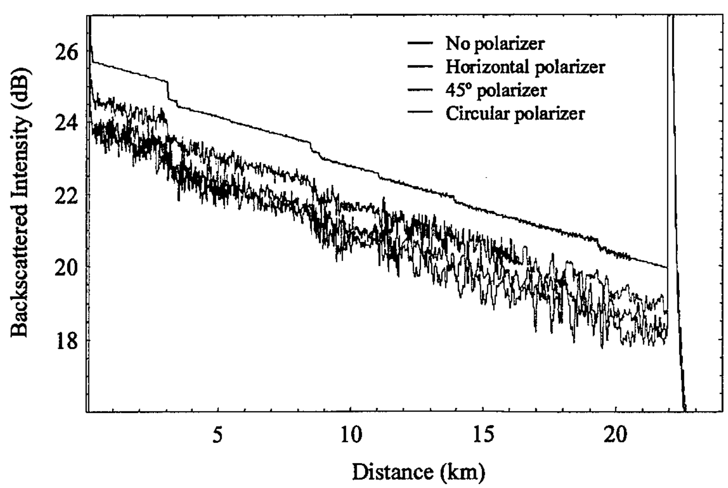

Wavelength: 1550 nm Pulsewidth: 275 ns

←.065→←.033→←.033→←.229→

PMD measured before fiber installation (ps/km$^{1/2}$)

Data set: WMR5D31
AT&T 5D fiber in *Lightpack* cable

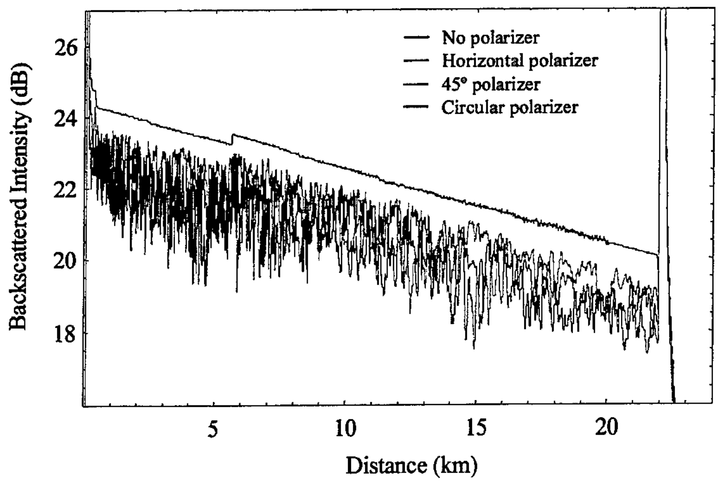

Wavelength: 1550 nm Pulsewidth: 275 ns

← .065 →← .065 →← .098 →← ??? →
PMD measured before fiber installation (ps/km$^{1/2}$)

Data set: WMR5D43
AT&T 5D fiber in *Lightpack* cable

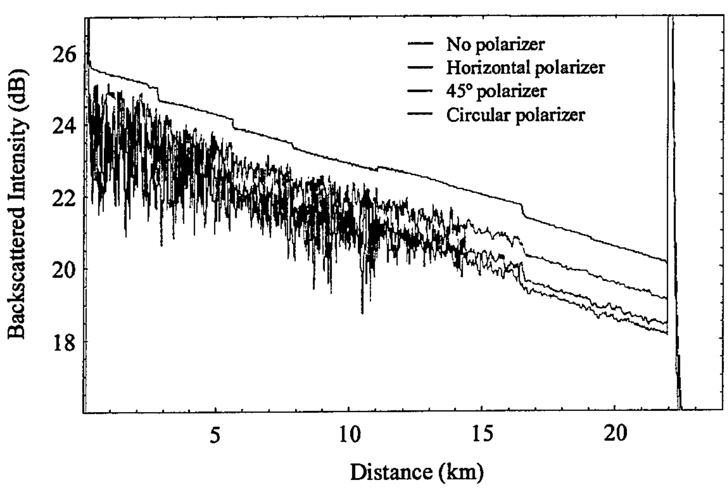

Wavelength: 1550 nm Pulsewidth: 275 ns

← .098 →← .033 →← .033 →← .261 →
PMD measured before fiber installation (ps/km$^{1/2}$)

Data set: WMR5D45
AT&T 5D fiber in *Lightpack* cable

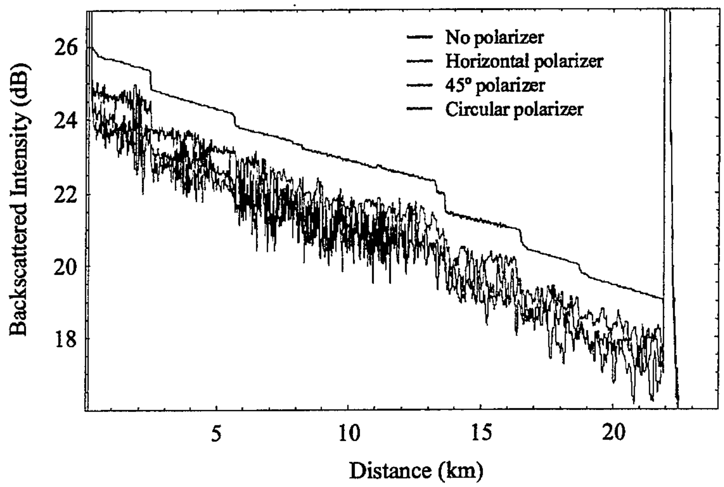

Wavelength: 1550 nm Pulsewidth: 275 ns

← .131 →← .033 →← .033 →← ??? →
PMD measured before fiber installation (ps/km$^{1/2}$)

Data set: WMR5D47
AT&T 5D fiber in *Lightpack* cable

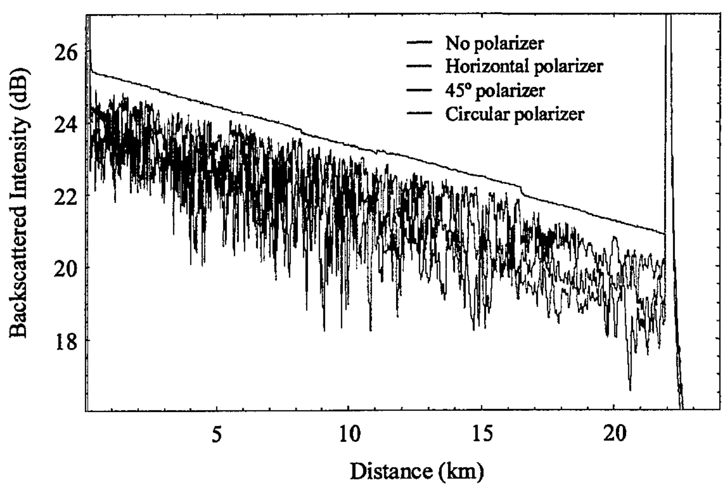

Wavelength: 1550 nm Pulsewidth: 275 ns

← ??? →← .098 →← .033 →← .033 →
PMD measured before fiber installation (ps/km$^{1/2}$)

Data set: WMR5D49
AT&T 5D fiber in *Lightpack* cable

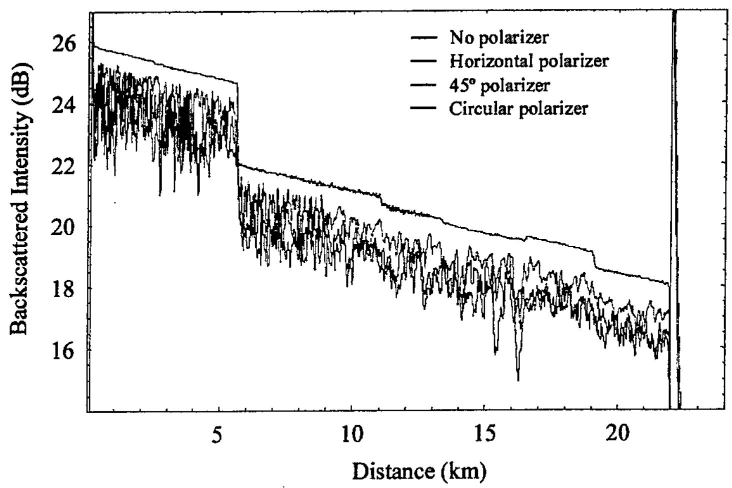

Wavelength: 1550 nm Pulsewidth: 275 ns

← .098 →← .033 →← .000 →← .033 →

PMD measured before fiber installation (ps/km$^{1/2}$)

Data set: R5D23
AT&T 5D fiber in ribbon NM cable

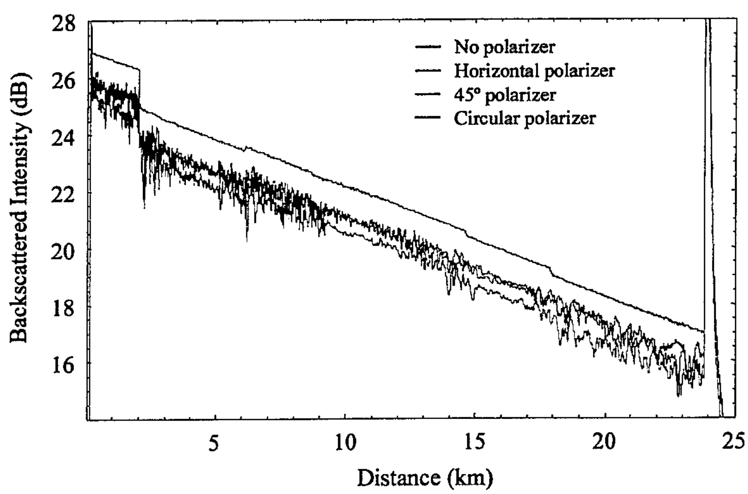

Wavelength: 1310 nm Pulsewidth: 275 ns

Data set: R5D25
AT&T 5D fiber in ribbon NM cable

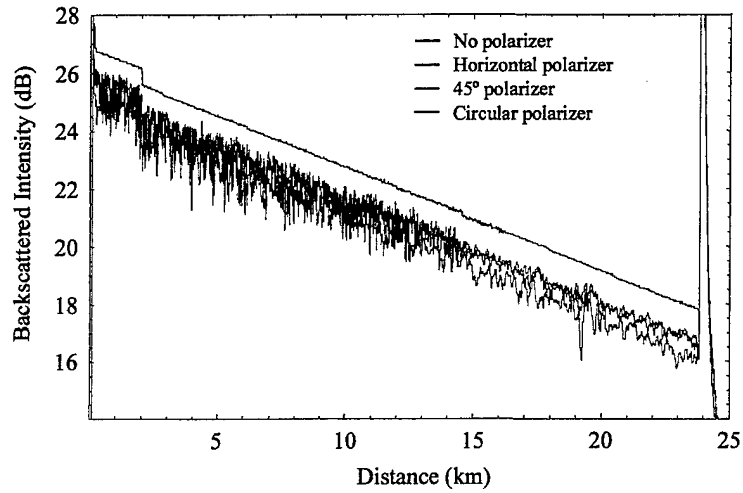

Wavelength: 1310 nm Pulsewidth: 275 ns

Data set: R5D27
AT&T 5D fiber in ribbon NM cable

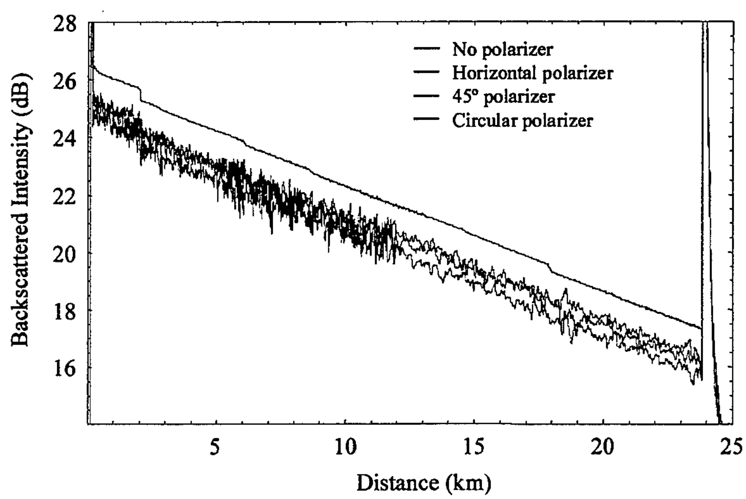

Wavelength: 1310 nm Pulsewidth: 275 ns

Data set: WMDSF13
AT&T dispersion-shifted (DEB) fiber in *Lightpack* cable

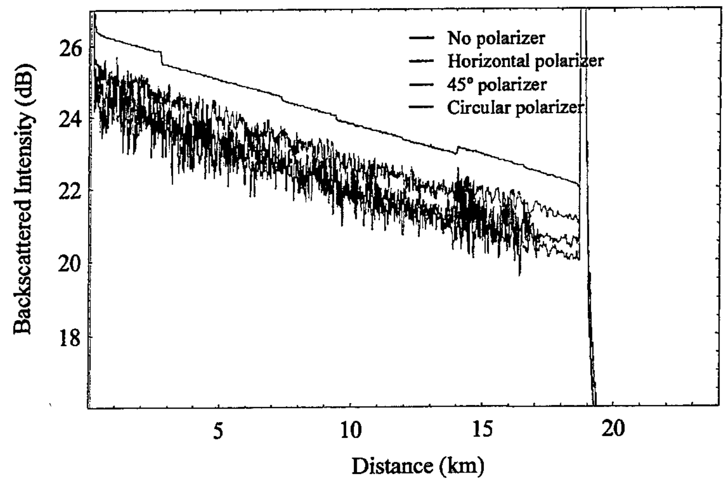

Wavelength: 1550 nm   Pulsewidth: 275 ns

Data set: WMDSF19
Corning dispersion-shifted fiber in *Lightpack* cable

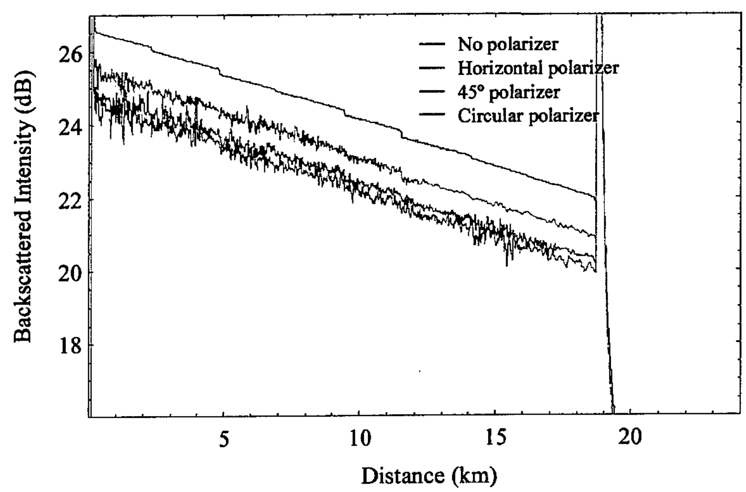

Wavelength: 1550 nm   Pulsewidth: 275 ns

Data set: WG1
AT&T low PMD fiber on a spool

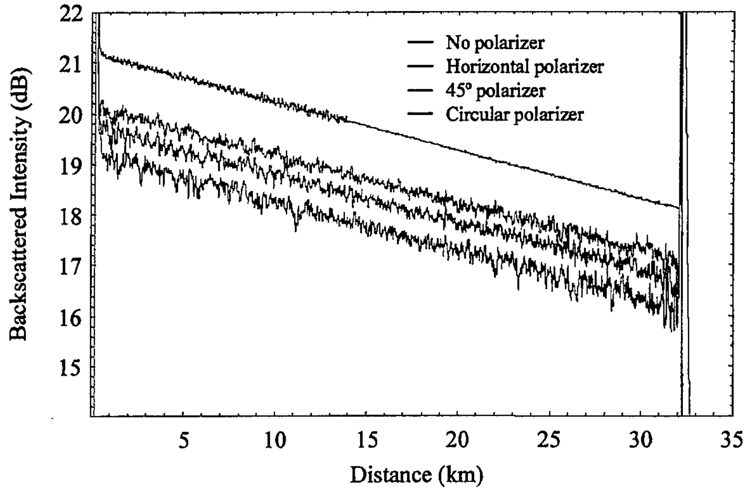

Wavelength: 1550 nm Pulsewidth: 275 ns